


 Cite this: *RSC Adv.*, 2024, 14, 34996

Enhancing skin delivery of tranexamic acid *via* esterification: synthesis and evaluation of alkyl ester derivatives†

 Yutong Zeng,^a Mengrui Ma,^{bc} Yongfeng Chen,^c Huichao Xie,^a Pingtian Ding^{*ac} and Keda Zhang^{*a}

Tranexamic acid (TA) is widely used clinically as a skin whitening agent for treating melasma and hyperpigmentation. However, oral administration of TA is often associated with adverse effects. Topical application could mitigate these issues, but the hydrophilic nature of TA limits its topical use. To overcome this limitation, we explored the design of TA alkyl ester prodrugs to enhance skin absorption. Our study specifically focused on the butyl and octyl ester derivatives of TA. The results demonstrated that TA4 and TA8 significantly improved skin penetration and deposition, by approximately 2–3 times compared to unmodified TA. Furthermore, these derivatives were rapidly hydrolyzed to release the parent drug within less than 2 h in both skin homogenates and blood. Safety assessments indicated no significant skin irritation in mice and revealed low cytotoxicity in HaCaT cells when exposed to the TA ester derivatives. We also developed a hydrogel formulation incorporating the TA derivatives, using hydroxyethyl cellulose, propylene glycol, Tween 80, and chlorobutanol. This formulation exhibited good skin absorption, stability, and user experience, making it a promising candidate for topical application. To sum up, the alkyl esterification prodrug design provides a promising approach for enhancing the skin delivery of TA.

 Received 30th August 2024
 Accepted 22nd October 2024

DOI: 10.1039/d4ra06266c

rsc.li/rsc-advances

1. Introduction

Melasma is a common skin condition characterized by the appearance of dark, discolored patches on the skin, primarily affecting areas exposed to the sun.¹ While the exact etiology of melasma remains elusive, it is widely believed to stem from an overproduction of melanin by melanocytes in the epidermis.^{2,3} Various factors, including ultraviolet (UV) exposure, hormonal changes, and genetic predisposition, are thought to contribute to this condition.³ Tranexamic acid (TA), traditionally used as an antifibrinolytic agent, has emerged as a promising treatment for melasma due to its ability to inhibit melanin synthesis.⁴ TA exerts its effects by acting as a tyrosinase inhibitor and interfering with the interaction between melanocytes and keratinocytes, thereby reducing melanin production.⁵

TA can be taken orally to achieve systemic skin-whitening effects.⁶ However, this method requires a medical prescription and supervision due to potential systemic side effects such as gastrointestinal disturbances and thromboembolic events. The

long-term safety of oral TA remains a concern, necessitating careful patient monitoring.^{7,8} Alternatively, dermatologists may inject TA directly into hyperpigmented areas.⁹ While this method allows for targeted delivery, it must be performed by trained professionals. The procedure carries risks of bruising, infection, and discomfort due to skin puncture. In addition, TA is commonly applied as creams, serums, or lotions directly to the skin.¹⁰ This route is favoured for its ease of use and reduced risk of systemic side effects. However, TA's highly hydrophilic nature, with its amino (–NH₂) and carboxylic acid (–COOH) groups, limits its ability to penetrate deeply into the skin where melanocytes reside.¹¹

Previous studies have demonstrated that prodrug modifications targeting the amino or carboxyl groups of tranexamic acid (TA) can modify its zwitterionic properties, increase its lipophilicity, and consequently improve its bioavailability. For instance, Svahn *et al.* performed a series of prodrug modifications by esterifying the carboxyl group with acyloxymethyl groups to enhance oral absorption.¹² Karaman *et al.* designed and synthesized maleamic acid amide derivatives to improve bioavailability, particularly oral absorption, while enabling sustained *in vivo* release of the parent drug, TA.¹³ However, due to the differences between the skin barrier and gastrointestinal mucosa, as well as the distinct pharmacokinetic profiles associated with topical *versus* oral administration, the suitability of these prodrugs for topical skin delivery remains uncertain. An

^aCollege of Pharmacy, Shenzhen Technology University, Shenzhen 518118, China. E-mail: dingpingtian@sztu.edu.cn; zhangkeda@sztu.edu.cn

^bQilu Pharmaceutical Co., Ltd, Jinan 250100, China

^cSchool of Pharmacy, Shenyang Pharmaceutical University, Shenyang 110016, China

 † Electronic supplementary information (ESI) available. See DOI: <https://doi.org/10.1039/d4ra06266c>


earlier patent introduced alkyl esters of TA as oil-soluble derivatives, which were empirically believed to be more readily absorbed through the skin, thereby enhancing the efficacy of topical treatments.¹⁴ Its clinical data confirmed that topical application of TA alkyl esters resulted in a depigmenting effect. However, another clinical study reported that both TA and its ethyl ester exhibited similar depigmenting effects when applied topically. This outcome contradicted initial expectations that the ethyl ester, being more readily absorbed, would demonstrate superior therapeutic effects. These observations underscore the necessity for further investigation into the pharmacokinetics and *in vitro* stability of TA alkyl esters in topical applications.

In this study, we emphasized the molecular design of TA alkyl esters, with a focus on their *in vitro* stability, skin absorption, metabolism, and safety profile. Additionally, a gel formulation incorporating these TA derivatives was developed to facilitate topical application. This study aimed to provide a scientific basis for the use of TA alkyl esters in enhancing skin delivery of TA and improving the treatment of melasma.

2. Materials and methods

2.1. Materials

TA, dichloromethane, methyl *tert*-butyl ether, thionyl chloride, methanol, acetonitrile, potassium dihydrogen phosphate, dipotassium hydrogen phosphate, *n*-butanol, and *n*-octanol were purchased from Sigma-Aldrich (Schnellendorf, Germany). Acetate ammonium, formic acid, hydroxyethyl cellulose (HEC), chlorobutanol, propylene glycol and Tween 80 were supplied by Kemiou (Tianjin, China). Diphenhydramine was obtained from National Institutes for Food and Drug Control (Beijing, China). Paraformaldehyde fixative (4%) and saline were purchased from Aladdin (Shanghai, China). All reagents were of the highest purity available but at least of analytical reagent grade.

2.2. Animals

Female Sprague-Dawley (SD) rats weighing 180–220 g and Kunming (KM) mice weighing 20–22 g were obtained from the Experimental Animal Center of Shenyang Pharmaceutical University (Shenyang, China). Upon arrival, the animals were allowed to acclimatize to the laboratory conditions for one week. All experimental protocols were approved by the Animal Ethics Committee of Shenyang Pharmaceutical University and were conducted in strict accordance with the Guide for the Care and Use of Laboratory Animals of China.

2.3. LEFR analysis

The following LEFR equation proposed by Zhang *et al.* was utilized to predict the skin permeability coefficients (K_p in cm s^{-1}) of ionized derivatives:¹⁵

$$\log K_p = -0.5328 + 0.137E - 0.604S - 0.338A - 2.428B - 1.797V - 1.4285J^+ + 2.471J^- \quad (1)$$

Here, the solute descriptors, E , S , A , B and V , represent the excess molar refractivity in units of $(\text{cm}^3 \text{mol}^{-1})/10$, dipolarity/polarizability, overall hydrogen bond acidity, overall hydrogen bond basicity, and McGowan volume in units of $(\text{cm}^3 \text{mol}^{-1})/100$, respectively. J^+ and J^- are the two ionic descriptors that refer to additional interactions involving cations and anions, respectively. The descriptors for neutral molecules were estimated using the Absolv module in ACD/Percepta (ACD/Labs, Toronto, Canada). We used the empirical equations proposed by Abraham and Acree to estimate the descriptors for protonated base cations from those for the corresponding neutral molecules.¹⁶ Once descriptors are known, the $\log K_p$ can be calculated using eqn (1).

2.4. Molecular docking

For the docking studies, human carboxylesterase (hCE1; PBD: 1MX1) was selected as the target enzyme to evaluate the binding interactions of the TA derivatives.¹⁷ The docking simulations were conducted using AMDock 1.4, a molecular docking software that facilitates the prediction of ligand–enzyme interactions.¹⁸ hCE1, a key enzyme involved in the hydrolysis of ester-based compounds, was chosen due to its relevance in the metabolic processing of TA derivatives.¹⁹

2.5. Synthesis of TA derivatives

The ester derivatives of TA, specifically the butyl ester (TA4) and octyl ester (TA8), were synthesized using the acyl chloride method, see Fig. 1. The procedure began with the dissolution of 3.14 g of TA in 150 mL of dichloromethane in a 250 mL three-neck round-bottom flask. The solution was stirred vigorously while maintaining the temperature with an ice bath. Under these conditions, 2.04 mL of thionyl chloride was added dropwise to the solution. The mixture was then allowed to react at 25 °C for 12 h, ensuring complete conversion to the acyl chloride intermediate. Following this, either 2.75 mL of *n*-butanol or 4.71 mL of *n*-octanol was introduced into the reaction mixture, depending on the desired ester derivative. The reaction proceeded for an additional 24 h to facilitate the esterification process. After the reaction, the organic solvent was removed using a vacuum rotary evaporator. This process yielded a white solid, which was further purified by washing with 200 mL of cold methyl *tert*-butyl ether. The solid was then isolated by filtration and subjected to vacuum drying for 48 h to obtain the final ester products. The yields of TA4 and TA8 are 92.33% and

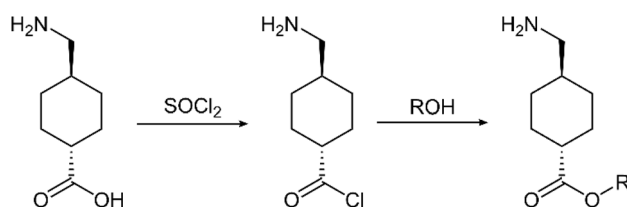


Fig. 1 Synthesis route of ester derivatives of TA. R represents an alkyl group (e.g., a butyl or octyl group).

89.62%, respectively. The synthesized compounds, TA4 and TA8, were characterized using $^1\text{H-NMR}$, $^{13}\text{C-NMR}$, and MS.

TA4: $^1\text{H-NMR}$ (600 MHz, CDCl_3) δ 8.35 (s, 3H), 4.06 (t, $J = 6.6$ Hz, 2H), 2.95–2.74 (m, 2H), 2.24 (tt, $J = 12.2, 3.5$ Hz, 1H), 2.05 (d, $J = 11.1$ Hz, 2H), 1.98 (d, $J = 11.1$ Hz, 2H), 1.86–1.70 (m, 1H), 1.60 (dt, $J = 14.5, 6.7$ Hz, 2H), 1.48 (qd, $J = 13.2, 3.2$ Hz, 2H), 1.42–1.31 (m, 2H), 1.14–1.00 (m, 2H), 0.93 (t, $J = 7.4$ Hz, 3H). $^{13}\text{C-NMR}$ (151 MHz, MeOD) δ 175.80, 63.83, 44.64, 42.6, 35.34, 30.34, 28.7, 27.84, 18.68, 12.52. LC-MS (ESI $^+$) m/z 214.1 $[\text{M} + \text{H}]^+$.

TA8: $^1\text{H-NMR}$ (600 MHz, D_2O) δ 3.98 (t, $J = 6.8$ Hz, 2H), 2.81 (d, $J = 7.1$ Hz, 2H), 2.23 (tt, $J = 12.2, 3.4$ Hz, 1H), 1.91 (d, $J = 11.2$ Hz, 2H), 1.84 (d, $J = 11.2$ Hz, 2H), 1.67–1.59 (m, 1H), 1.58–1.48 (m, 2H), 1.36 (qt, $J = 22.3, 11.2$ Hz, 2H), 1.30–1.10 (m, 10H), 0.99 (qd, $J = 13.0, 3.2$ Hz, 2H), 0.80 (t, $J = 6.9$ Hz, 3H). $^{13}\text{C-NMR}$ (151 MHz, MeOD) δ 175.79, 64.11, 44.64, 42.60, 35.24, 31.45, 28.83, 28.70, 28.70, 28.23, 27.85, 25.52, 22.20, 12.93. LC-MS (ESI $^+$) m/z 270.2 $[\text{M} + \text{H}]^+$.

2.6. Melting points of derivatives

The melting points of TA, TA4, and TA8 were determined using a Mettler Toledo DSC1 differential scanning calorimeter (Zurich, Switzerland). Accurately weighed quantities of each compound were placed into separate crucibles. A blank crucible was utilized as a control to ensure baseline accuracy during the measurements. The differential scanning calorimetry (DSC) analysis was conducted over a temperature range from 25 °C to 250 °C, with a heating rate of 10 °C min^{-1} .

2.7. Stability test of derivatives

The stability of TA ester derivatives in aqueous solutions across different pH levels was investigated over a 72 h period at 37 °C. Phosphate-buffered saline (PBS) solutions of TA derivatives were prepared at a concentration of 100 $\mu\text{g mL}^{-1}$, spanning a pH range from 5.0 to 7.4. These solutions were placed in a thermostatic shaker set at 37 °C and sampled at 0, 24, 48, and 72 h. The concentrations of the derivatives were measured using high-performance liquid chromatography (HPLC).

The stability of TA derivatives in rat skin homogenates was studied using SD rats. Rats were anesthetized with an intraperitoneal injection of urethane (1.5 g kg^{-1}). After hair removal by depilatory cream, skin samples were harvested and rinsed with 4 °C saline to remove blood. The skin was homogenized on ice with a ratio of 1 g skin to 4 mL saline, using an IKA $^{\text{®}}$ T18 Ultra-Turrax homogenizer (Staufen, Germany). The homogenate was centrifuged at 3000 rpm for 10 min, and the supernatant was stored at -20 °C until use. For the stability assessment, 100 μL of a 100 $\mu\text{g per mL}$ TA derivative solution was mixed with 900 μL of the skin homogenate supernatant. The mixture was incubated at 37 °C, with 40 μL samples taken at 0, 20, 50, 80, 120, and 150 min. An equal volume of blank skin homogenate supernatant was added after each sampling. The collected samples were treated with cold methanol at a ratio of 1 : 4 (v/v) for protein precipitation and centrifuged at 13 000 rpm for 5 min. The supernatant was then prepared for analysis by mixing with 10 μL of diphenhydramine as an internal standard and 140 μL of 5 mM ammonium acetate containing 0.1% formic

acid. The processed samples were analyzed for drug concentration using liquid chromatography-tandem mass spectrometry (LC-MS/MS), as detailed in the ESI. \dagger

The stability of TA derivatives in plasma was assessed by collecting blood from the orbital sinus of SD rats. The blood was centrifuged at 3000 rpm for 10 min to separate the plasma. 50 μL of a 100 $\mu\text{g per mL}$ TA derivative solution was mixed with 950 μL of blank plasma. The samples were incubated in a 37 °C thermostatic water bath shaker, and 40 μL aliquots were taken at 0, 5, 10, 15, 20, and 25 min. An equal volume of blank plasma was added after each sampling. Protein precipitation was carried out by adding cold methanol. The samples were centrifuged, and the supernatant was collected for LC-MS/MS analysis to determine the drug concentration.

2.8. *In vitro* skin permeation study

Skin permeation experiments were performed using Franz diffusion cells. Fresh porcine skin, sourced from Jingde Agricultural (Hebei, China), were depilated, and the subcutaneous fatty tissues were carefully removed using scalpels. The resulting full-thickness skin was washed with physiological saline, and stored at -20 °C until use. During experiments, the skin samples were mounted on Franz diffusion cells with an effective diffusion area of 3.14 cm^2 . The receptor chamber of each cell was filled with 7 mL of physiological saline, and the donor chamber was filled with 2 mL of 20 mM solutions of TA, TA4, or TA8. The diffusion cells were maintained at 32 °C using a water bath. A 0.7 mL aliquot was withdrawn from the receptor chamber every 2 h over a 12 h period, and an equal volume of fresh saline was added immediately after each sampling. Each experiment was performed in triplicate. The collected samples underwent protein precipitation with cold methanol and were analyzed using LC-MS/MS. Due to the hydrolysis of TA4 and TA8 in the skin, their quantification encompasses these compounds themselves and the hydrolysis product, TA.

To evaluate the deposition of TA and its derivatives within the skin, the treated skin samples were collected following the permeation experiments. The excised skin tissues were finely minced and placed into EP tubes containing an appropriate volume of saline. These samples were homogenized and subsequently transferred into 10 mL volumetric flasks. The volume was adjusted to 10 mL using physiological saline. The homogenate was then subjected to centrifugation at 13 000 rpm for 10 min. The supernatant was collected and underwent protein precipitation. Finally, the processed supernatant was analyzed for drug concentration using LC-MS/MS.

2.9. Gel formulation and evaluation

The formulation of the TA8 gel was developed using HEC as the gelling agent, propylene glycol as a moisturizer, Tween 80 as a lubricant, and chlorobutanol as a preservative. To prepare the gel, chlorobutanol was first dissolved in 50% of the total volume of deionized water, heated to 70 °C, and subsequently cooled to room temperature. The gel matrix was then created by incorporating the prescribed amount of HEC into the cooled chlorobutanol solution, followed by thorough stirring and a standing

period of 0.5 to 1 h to ensure complete hydration and gel formation. In a separate step, the specified quantity of TA8 was dissolved in a mixture of propylene glycol and 25% deionized water. Tween 80 was then added to this solution, and the final volume was adjusted with additional deionized water. The mixture was stirred until it reached a homogenous state. To identify the optimal HEC concentration for the gel matrix, formulations containing TA8 were prepared with varying HEC concentrations of 1.3%, 1.5%, 1.7%, and 2.0%. These samples were allowed to equilibrate for 24 h before being subjected to rheological analysis. Rheological properties were measured at 25 °C using an AR 2000ex rheometer (TA Instruments, Eschborn, Germany). Further optimization of the gel formulation was conducted through single-factor experiments. The concentrations of HEC were kept constant while the quantities of propylene glycol (7.5%, 10.0%, and 12.5%) and Tween 80 (0.5%, 1.0%, and 1.5%) were varied to examine their effects on the gel properties. Each formulation underwent a 10 h *in vitro* skin permeation test, where 1 g of gel was uniformly applied to the porcine skin. The concentrations of TA8 and its metabolite TA in the receptor fluid were measured as described previously. The measurements were then used to determine the optimal concentrations of propylene glycol and Tween 80 in the formulation.

2.10. Gel stability test

The stability study was conducted for TA8 gel. Three batches of TA8 gel were packaged in medical-grade aluminum tubes, and then placed in an LRH250Y drug stability test chamber (Taihong Medical, China), maintained at a constant temperature of 30 ± 2 °C and a relative humidity of $65 \pm 5\%$ for a period of 6 months. Samples were taken at the end of the 1st, 3rd, and 6th months. After diluting appropriately, samples were analyzed using HPLC.

2.11. Skin irritation study

This study evaluated the potential of TA8 gel to cause skin irritation using the Draize test method on KM mice.²⁰ Eight KM mice were divided into two groups: a single-dose group and

a multiple-dose group, each containing four mice. Specifically, one day before the administration, the dorsal region of mice was depilated using an electric clipper. On the dorsal skin, one area (1.0 cm × 1.0 cm) was marked on both sides of the spine. In the single-dose test, 0.3 g of TA8 gel was applied to the right designated skin area on each mouse. The left area, serving as a control, received 0.3 g of a blank gel. Skin reactions (erythema, eschar formation, and edema) were observed and scored according to the Draize scoring system at 1, 24, 48, and 72 h after administration. For the multiple-dose test, TA8 gel was applied daily to the right designated area of the dorsal skin for 14 consecutive days. Prior to each daily application, skin reactions were assessed and scored to evaluate the cumulative irritation. The mean scores of skin reactions were used to determine the presence and intensity of skin irritation. One day after the completion of the dosing period, the mice were euthanized, and skin samples from the application sites were excised for histopathological examination.

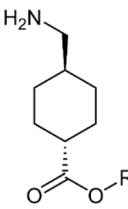
2.12. *In vitro* cytotoxicity assay

The cytotoxicity of TA8 on HaCaT cells was evaluated using the Cell Counting Kit-8 (CCK-8) assay. HaCaT cells were seeded into 96 well plates at a density of 10 000 cells per well. The cells were incubated with varying concentrations of TA8 for 12 hours. A drug-free medium served as the control. After incubation, the cells were washed twice with PBS and stained with CCK-8 reagent (10% in serum-free medium) for 1 h. The absorbance of each well was measured using a microplate reader to quantify cell viability.

3. Results and discussion

In this study, the alkyl esterification prodrug strategy was proposed to enhance the skin absorption of TA. To optimize the carbon chain length for modification, we utilized ACD/Percepta software to calculate the $\log P_{o/w}$ values of TA derivatives with varying chain lengths (see Table 1). Generally, compounds with a moderate $\log P_{o/w}$ (ranging from 0 to 5) and a molecular weight (MW) below 500 Da are more likely to permeate the stratum

Table 1 Physicochemical parameters of TA and its ester derivatives

Structure	R group	Compound	MW	pK _a ^a	Log P _{o/w}	E _i	S _i	A _i	B _i	V _i	J ⁺	J ⁻	log K _p ^c
	-H	TA	157.21	10.66	0.26	N/A ^b	N/A ^b	N/A ^b	N/A ^b	N/A ^b	N/A ^b	N/A ^b	N/A ^b
	-CH ₃	TA1	171.24	10.38	0.86	0.34	2.99	2.21	0.00	1.4615	0.8395	0.00	-6.46
	-CH ₂ CH ₃	TA2	185.26	10.38	1.74	0.34	3.02	2.21	0.00	1.6015	0.8507	0.00	-6.24
	-(CH ₂) ₂ CH ₃	TA3	199.29	10.38	2.3	0.33	3.01	2.21	0.00	1.7415	0.8407	0.00	-5.97
	-(CH ₂) ₃ CH ₃	TA4	213.32	10.38	2.56	0.33	3.01	2.23	0.00	1.8915	0.8328	0.00	-5.69
	-(CH ₂) ₄ CH ₃	TA5	227.34	10.38	2.85	0.33	3.04	2.23	0.00	2.0315	0.8441	0.00	-5.47
	-(CH ₂) ₅ CH ₃	TA6	241.37	10.38	3.34	0.33	3.04	2.24	0.00	2.1715	0.8361	0.00	-5.21
	-(CH ₂) ₆ CH ₃	TA7	255.4	10.38	4.27	0.33	3.04	2.24	0.00	2.3115	0.8361	0.00	-4.96
	-(CH ₂) ₇ CH ₃	TA8	269.42	10.38	4.75	0.33	3.06	2.26	0.00	2.4515	0.8395	0.00	-4.74
-(CH ₂) ₈ CH ₃	TA9	283.45	10.38	4.95	0.32	3.06	2.26	0.00	2.5915	0.8294	0.00	-4.47	

^a Calculated using the GALAS algorithm in ACD/Percepta. ^b Not applicable for zwitterions; the value cannot be obtained due to the zwitterionic property. ^c K_p in cm s⁻¹; the values are specific to ionized compounds.

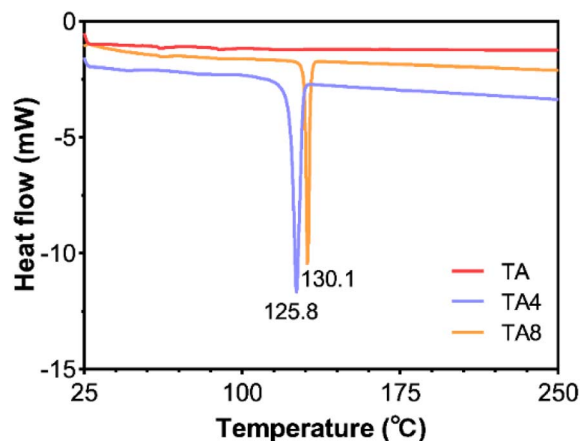


Fig. 2 DSC curves of TA and its derivatives in the range of 25–250 °C.

corneum and reach the viable epidermis and dermis.²¹ Based on these criteria, the C1–C9 ester derivatives of TA were identified as suitable candidates. However, these derivatives contain primary amine groups with pK_a values greater than 10.0, leading to their almost complete ionization (>99.9%) at the pH range of the skin and topical formulations (pH 4.0–7.0). Given that ionization can significantly impact the ability of a compound to penetrate the skin, we calculated the $\log K_p$ values for the cations from protonated TA derivatives using the LFER equation,¹⁵ as shown in Table 1. The results demonstrated that the $\log K_p$ of the ionized TA derivatives increased with the length of the carbon chain, ranging from -6.46 for the C1 derivative to -4.47 for the C9 derivative. According to our previous study,²² a $\log K_p$ value exceeding -7.0 is an empirical threshold indicating the potential of a compound for effective skin

penetration. Therefore, these nine TA derivatives are predicted to possess favorable skin permeation properties when applied topically.

To reduce the synthesis workload, the butyl ester (TA4) and octyl ester (TA8) derivatives of TA were chosen as our study subjects. TA4 and TA8 were synthesized through acyl chloride esterification, and their structures were characterized using HNMR, CNMR, and MS (see Fig. S1 and S2†). DSC analysis revealed the melting points of TA4 and TA8 to be 125.8 °C and 130.1 °C, respectively, as shown in Fig. 2. TA itself did not exhibit a melting endotherm in the range of 25–250 °C, indicating that its melting point exceeds 250 °C, consistent with existing reports.²³ The significantly lower melting points of the TA ester derivatives compared to the parent TA are in line with theoretical expectations. Esterification reduces the intermolecular hydrogen bond interaction, leading to a decrease in melting point. Compounds with lower melting points generally have weaker intermolecular forces and tend to behave more ideally in solution, resulting in higher thermodynamic activity and better skin permeability.²⁴ Therefore, the observations regarding the melting points are in agreement with our previous calculations on skin permeability, supporting their potential as effective prodrugs for improving the skin absorption of TA. We investigated the stability of TA ester derivatives (TA4 and TA8) under various pH conditions. In both saline and aqueous solutions with pH values ranging from 5.0 to 7.4, TA4 and TA8 exhibited minimal concentration changes over 72 h (see Fig. 3A). This suggests that these derivatives are resistant to hydrolysis under such conditions. In contrast, in biological samples such as skin homogenates and plasma, the levels of TA4 and TA8 decreased rapidly (Fig. 3B). This decline is likely due to esterase-mediated hydrolysis, which is prominent in

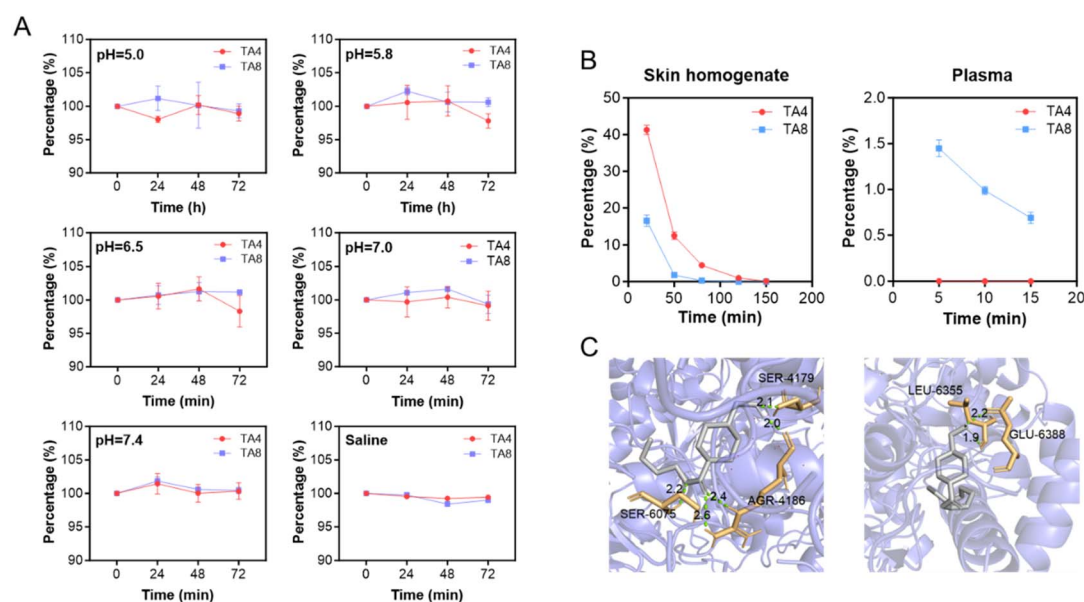


Fig. 3 Stability of TA derivatives in aqueous solution, skin homogenate and plasma. (A) Concentration changes of TA derivatives in PBS solution under different pH conditions. (B) Concentration changes of TA derivatives in skin homogenate and plasma. (C) *In silico* docking simulation of TA derivatives and hCE1 using AMDock software.

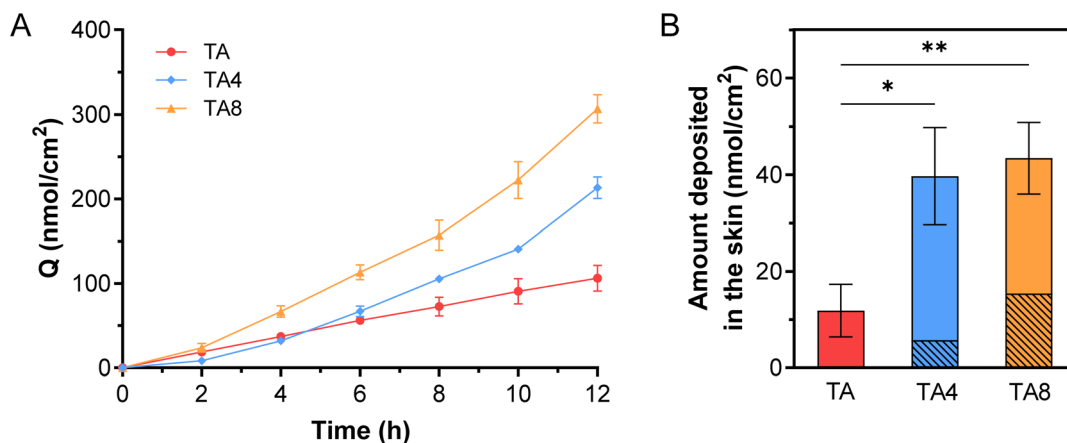


Fig. 4 Skin penetration and deposition of TA and its ester derivatives. (A) Cumulative amount of each compound permeated (Q) through porcine skin over 12 h ($n = 4$). (B) Amount of each compound deposited in the skin after skin permeation experiments ($n = 4$). The diagonally lined portion of the bar graph indicates the amount of TA generated from the hydrolysis of TA derivatives in the skin. * $p < 0.05$, ** $p < 0.01$.

these biological environments.²⁵ Generally, esterases exhibit high catalytic efficiency, with hydrolysis rates that can be several orders of magnitude faster than non-enzymatic reactions.²⁶ Thus, it is possible to achieve nearly complete hydrolysis of some esters by esterases within minutes, especially under optimal conditions. Similar observations have been reported in the literature, such as the rapid hydrolysis of various ester prodrugs of ibuprofen and flurbiprofen in human plasma and ester prodrugs of naltrexone in skin homogenates.^{27,28}

To understand the interaction between TA derivatives and human carboxylesterases, we performed molecular docking simulations using AMDock 1.4 software. The simulations modeled the interactions of TA derivatives with hCE1, the major esterase expressed in human skin.¹⁹ The results, presented in Fig. 3C, showed that TA4 forms hydrogen bonds with the AGR-4186, SER-6075, and SER-4179 residues of hCES1, while TA8 forms hydrogen bonds with the GLU-6388 and LEU-6355 residues. The lowest binding energies for TA4 and TA8 were $-31.25 \text{ kJ mol}^{-1}$ and $-31.80 \text{ kJ mol}^{-1}$, respectively. These low binding energies indicate a strong affinity of the TA ester derivatives for the esterase enzyme, corroborating our experimental observations. TA4 and TA8 were almost completely hydrolyzed in skin homogenates within 120 min and achieved similar levels of hydrolysis in plasma within 5 min. Additionally, TA8 underwent hydrolysis at a faster rate than TA4 in skin homogenates, whereas TA4 was hydrolyzed more rapidly than TA8 in plasma. These findings suggest that TA ester derivatives remain stability in topical formulations but are efficiently converted to the parent drug, TA, upon exposure to biological conditions.

The skin penetration and deposition profiles of TA and its derivatives were further examined, as shown in Fig. 4. The steady-state flux (J_s) of TA was found to be $8.80 \text{ nmol cm}^{-2} \text{ h}^{-1}$. In contrast, the J_s values for TA4 and TA8 were 2.15 and 3.12 times higher than that of TA, respectively, corresponding to 18.93 and $27.48 \text{ nmol cm}^{-2} \text{ h}^{-1}$ (Fig. 4A). The raw data were presented in Fig. S3–S5 and Table S1.† Additionally, the amount

of TA4 and TA8 deposited in the skin was 3.35 and 3.78 times greater than that of TA (Fig. 4B). Both TA4 and TA8 showed varying degrees of hydrolysis, with TA8 exhibiting higher hydrolysis rates, consistent with *in vitro* findings. It is worth noting that the hydrolysis of TA derivatives during the diffusion through the skin was less pronounced compared to the previous observations in skin homogenates. This discrepancy could be attributed to the use of non-fresh skin (*i.e.*, skin stored at -20°C) in the permeation experiments, which may have resulted in reduced or lost esterase activity. Overall, alkyl esterification significantly improved the skin absorption of TA, with substantial skin deposition facilitating local pharmacological effects.

For the ester derivatives of TA, we developed a hydrogel formulation containing HEC, propylene glycol, Tween 80, and chlorobutanol. Using 2% TA8 as the active ingredient, we optimized the ratio of each excipient in the formulation. The viscosity of the HEC-based gel matrix increases with HEC concentration but decreases with increasing shear rate, exhibiting shear-thinning behaviour characteristic of non-Newtonian pseudoplastic fluids (see Fig. 5A). During application, high shear stress reduces the viscosity of the gel, facilitating its spreading. Once application is complete, the viscosity increases under low shear stress, aiding in the gel's adhesion to the skin surface. Upon comparison, a 1.5% concentration of HEC was determined to provide the optimal viscosity for the gel system, and thus was selected as the optimal concentration. Propylene glycol acts as a humectant and disrupts the stratum corneum to promote drug absorption, typically used at 5–15%.²⁹ The water loss rates of gels containing 0–15% propylene glycol were evaluated, see Fig. S6.† When the humectant concentration reached 10%, further increases did not significantly affect the water loss rate. We further investigated the effects of 7.5–12.5% propylene glycol on the skin absorption of TA8. The permeation of TA8 increased with propylene glycol concentration up to 10%, beyond which no significant difference was observed (Fig. 5B). Given the potential skin irritation associated with high

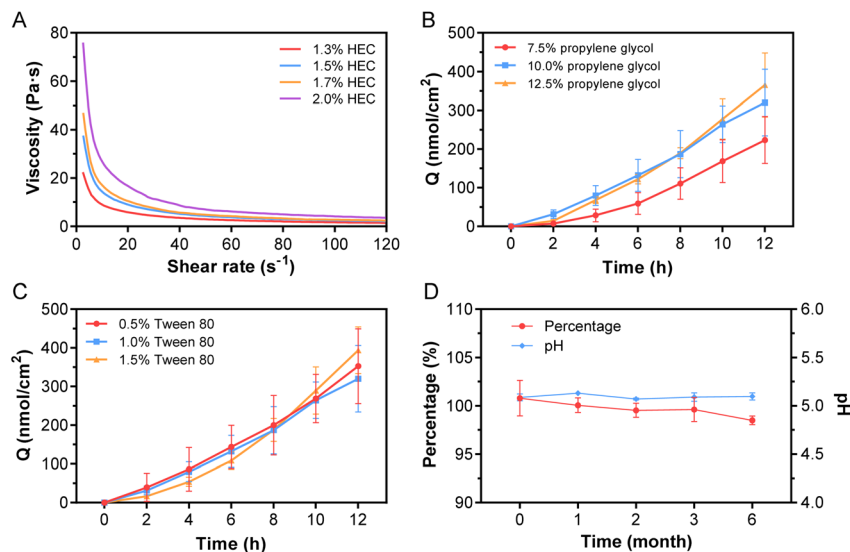


Fig. 5 Formulation optimization and stability evaluation of TA8 gel. (A) Viscosity curves of TA gels with varying concentrations of HEC. (B) Permeation profile of TA8 across porcine skin over 12 h for TA gels with different concentrations of propylene glycol ($n = 4$). (C) Permeation profile of TA8 across porcine skin over 12 h for TA gels with different concentrations of Tween 80 ($n = 4$). (D) Changes in TA8 concentration and pH of TA8 gel over a 6 months period.

Table 2 Formulation of TA8 gel

Ingredients	Concentration (w/w)
TA8	2%
HEC	1.50%
Propylene glycol	10%
Tween 80	1%
Chlorobutanol	0.25%
Deionized water	q.s. to make 100 g

concentrations of propylene glycol,³⁰ the optimal concentration was set at 10%. Tween 80 was incorporated to improve the spreadability of the gel. However, as a surfactant, its inclusion could potentially affect the skin absorption of TA8.³¹ We investigated the effect of Tween 80 concentrations ranging from 0.5% to 1.5% on the skin permeation of TA8. Tween 80 showed

minimal impact on the skin permeation of TA8 (Fig. 5C). Therefore, the appearance and spreadability of gel were used as evaluation criteria, settling on a Tween 80 concentration of 1%. Chlorobutanol serves as a neutral preservative, typically used in concentrations of 0.25% to 0.5%. Considering safety, we opted for a chlorobutanol concentration of 0.25%. Based on these comprehensive evaluations, the optimal formulation for the TA8 gel is detailed in Table 2. Additionally, the long-term stability of the TA8 gel was assessed. The results indicated that over a period of 6 months, the content of TA8 in the gel varied by less than 2%, and the pH remained relatively stable (Fig. 5D). This demonstrates that the designed TA8 hydrogel formulation possesses good stability.

Safety is a critical consideration in the development of pro-drugs. We assessed the skin toxicity of TA8 using HaCaT cells, a human keratinocyte cell line. TA8 exhibited no significant

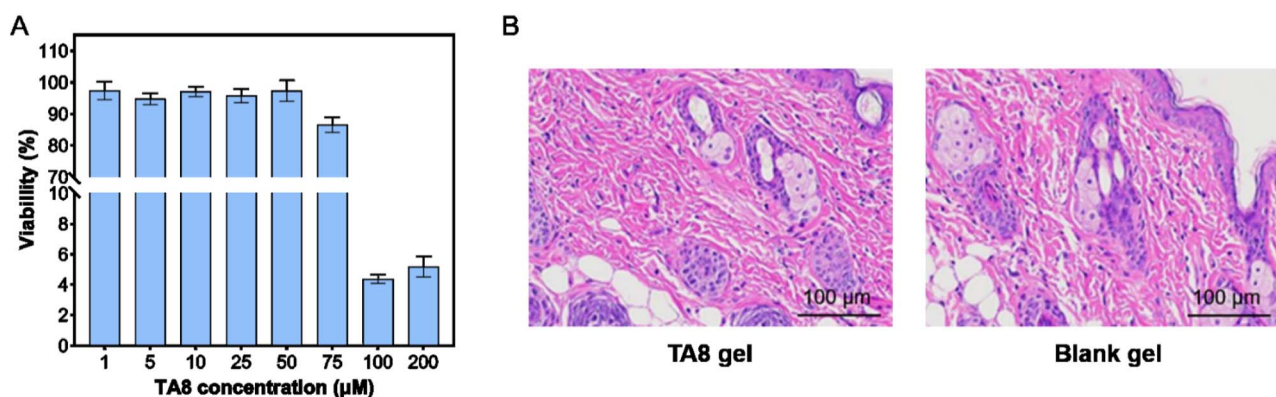


Fig. 6 Safety assessment of TA8 *in vivo* and *in vitro*. (A) Viability of HaCaT cells treated with TA8 at different concentrations. (B) Histopathological analysis (H&E staining) of mouse skin following 14 days of topical application of TA8 gel and blank gel.

cytotoxicity at concentrations below 75 μM (Fig. 6A), indicating a high safety margin. To further evaluate its safety profile, both acute and long-term skin irritation assessments were conducted using the Draize test on KM mice through single and multiple dosing. Both tests yielded irritation scores of zero, indicating no observable irritation. Histological analysis of the KM mice treated with TA8 gel revealed that the epidermal layer structure remained intact, with normal squamous epithelial cell morphology (Fig. 6B). The dermis exhibited a rich presence of collagen fibers, and the appendages, including hair follicles and sebaceous glands, were preserved and unaffected. Moreover, there was no evidence of inflammatory cell infiltration or any pathological changes. These results suggest that the gel formulation possesses good biocompatibility and that the TA8 component does not induce significant skin irritation, highlighting its potential as a safe prodrug for topical applications.

4. Conclusion

This study successfully developed TA prodrugs through alkyl esterification to alter its zwitterionic nature, increase lipophilicity, and enhance the skin absorption of TA. Our findings revealed that this strategy not only improved the skin penetration and deposition of TA as expected, but also allowed for rapid hydrolysis of the ester derivatives to release the parent drug once inside the skin, thereby ensuring its pharmacological efficacy. The TA ester derivatives demonstrated good stability and solubility in aqueous solutions (pH 5.0–7.0), making them suitable for topical formulation development. These derivatives exhibited no significant skin irritation and low cytotoxicity. For the TA ester derivatives, we developed a hydrogel formulation with suitable user experience, stability, and effective skin absorption. Overall, this study suggests that alkyl esterification is an effective strategy for enhancing the skin absorption of TA. Further studies will be done to optimize the prodrug structure for even greater skin absorption and minimal systemic exposure. Exploring different alkyl chain lengths and branching may yield derivatives with tailored pharmacokinetic profiles. Furthermore, the integration of nanostructured and smart delivery systems, such as liposomes and their analogues, could enhance penetration and release mechanisms, ultimately leading to improved patient outcomes in treating melasma and hyperpigmentation.

Data availability

The data supporting this article have been included as part of the ESI.†

Conflicts of interest

There are no conflicts of interest to declare.

Acknowledgements

This study was supported by the Graduate School's Collaborative Research of SZTU (Grant No. 20233108010006) and the

Natural Science Foundation of Top Talent of SZTU (Grant No. GDRC202305).

References

- 1 S. H. Kwon, J. I. Na, J. Y. Choi and K. C. Park, *Exp. Dermatol.*, 2019, **28**, 704–708.
- 2 O. Artzi, T. Horovitz, E. Bar-Ilan, W. Shehadeh, A. Koren, L. Zusmanovitch, J. N. Mehrabi, F. Salameh, G. Isman Nelkenbaum and E. Zur, *J. Cosmet. Dermatol.*, 2021, **20**, 3432–3445.
- 3 A. C. C. Espósito, D. P. Cassiano, C. N. da Silva, P. B. Lima, J. A. Dias, K. Hassun, E. Bagatin, L. D. Miot and H. A. Miot, *Dermatol. Ther.*, 2022, **12**, 1967–1988.
- 4 M. Perper, A. E. Eber, R. Fayne, S. H. Verne, R. J. Magno, J. Cervantes, M. Alharbi, I. Alomair, A. Alfuraih and K. Nouri, *Am. J. Clin. Dermatol.*, 2017, **18**, 373–381.
- 5 H. Konisky, E. Balazic, J. A. Jaller, U. Khanna and K. Kobets, *J. Cosmet. Dermatol.*, 2023, **22**, 1197–1206.
- 6 H. R. Bala, S. Lee, C. Wong, A. G. Pandya and M. Rodrigues, *Dermatol. Surg.*, 2018, **44**, 814–825.
- 7 H. J. Kim, S. H. Moon, S. H. Cho, J. D. Lee and H. S. Kim, *Acta Derm. Venereol.*, 2017, **97**, 776–781.
- 8 X. Feng, H. Su and J. Xie, *J. Clin. Pharm. Ther.*, 2021, **46**, 1263–1273.
- 9 A. Y. Badran, A. U. Ali and A. S. Gomaa, *Australas. J. Dermatol.*, 2021, **62**, e373–e379.
- 10 K. Maeda, *Cosmetics*, 2022, **9**, 108.
- 11 P. Verma and K. S. Yadav, *Expert Opin. Drug Delivery*, 2023, **20**, 773–783.
- 12 C. M. Svahn, F. Merenyi and L. Karlson, *J. Med. Chem.*, 1986, **29**, 448–453.
- 13 R. Karaman, H. Ghareeb, K. K. Dajani, L. Scranio, H. Hallak, S. Abu-Lafi, G. Mecca and S. A. Bufo, *J. Comput.-Aided Mol. Des.*, 2013, **27**, 615–635.
- 14 Nippon Saafuakutanto Kogyo KK, Tranexamic Ester and Antipigmentary External Agent with The Same as Active Ingredient, *Jpn Pat.*, JP04046144A, 1992.
- 15 K. Zhang, M. H. Abraham and X. Liu, *Int. J. Pharm.*, 2017, **521**, 259–266.
- 16 M. H. Abraham and W. E. Acree Jr, *J. Org. Chem.*, 2010, **75**, 1006–1015.
- 17 S. Bencharit, C. L. Morton, J. L. Hyatt, P. Kuhn, M. K. Danks, P. M. Potter and M. R. Redinbo, *Chem. Biol.*, 2003, **10**, 341–349.
- 18 M. S. Valdés-Tresanco, M. E. Valdés-Tresanco, P. A. Valiente and E. Moreno, *Biol. Direct*, 2020, **15**, 12.
- 19 D. Wang, L. Zou, Q. Jin, J. Hou, G. Ge and L. Yang, *Acta Pharm. Sin. B*, 2018, **8**, 699–712.
- 20 J. H. Draize, G. Woodard and H. O. Calvery, *J. Pharmacol. Exp. Ther.*, 1944, **82**, 377.
- 21 M. S. Roberts, H. S. Cheruvu, S. E. Mangion, A. Alinaghi, H. A. Benson, Y. Mohammed, A. Holmes, J. van der Hoek, M. Pastore and J. E. Grice, *Adv. Drug Delivery Rev.*, 2021, **177**, 113929.

- 22 K. Zhang, W. Sun, A. Fahr, X. Zeng, L. Ge, M. Chen, L. Yang, S. Wu, J. Fei and B. Zhou, *New J. Chem.*, 2019, **43**, 12538–12547.
- 23 P. W. Hsieh, W. Y. Chen, I. A. Aljuffali, C. C. Chen and J. Y. Fang, *Curr. Med. Chem.*, 2013, **20**, 4080–4092.
- 24 K. A. Chu and S. H. Yalkowsky, *Int. J. Pharm.*, 2009, **373**, 24–40.
- 25 K. Vávrová, A. Hrabálek, P. Doležal, T. Holas and J. Klimentová, *J. Controlled Release*, 2005, **104**, 41–49.
- 26 J. Fu, M. Sadgrove, L. Marson and M. Jay, *Drug Metab. Dispos.*, 2016, **44**, 1313.
- 27 H. Maag, in *Prodrugs: Challenges and Rewards Part 1*, ed. V. J. Stella, R. T. Borchardt, M. J. Hageman, R. Oliyai, H. Maag and J. W. Tilley, Springer New York, New York, NY, 2007, pp. 703–729.
- 28 D. C. Hammell, E. I. Stolarczyk, M. Klausner, M. O. Hamad, P. A. Crooks and A. L. Stinchcomb, *J. Pharm. Sci.*, 2005, **94**, 828–836.
- 29 H. L. Yu and C. F. Goh, *Eur. J. Pharm. Biopharm.*, 2024, **196**, 114182.
- 30 M. A. Pemberton and I. Kimber, *Regul. Toxicol. Pharmacol.*, 2023, **138**, 105341.
- 31 M. J. Cappel and J. Kreuter, *Int. J. Pharm.*, 1991, **69**, 143–153.